Obrabotka metallov (tekhnologiya, oborudovanie, instrumenty) = Metal Working and Material Science. 2021 vol. 23 no. 3 pp. 20–30
ISSN: 1994-6309 (print) / 2541-819X (online)
DOI: 10.17212/1994-6309-2021-23.3-20-30

NSTU NETI

Obrabotka metallov -
Metal Working and Material Science

Journal homepage: http://journals.nstu.ru/obrabotka_metallov

On the issue of selecting and optimizing parameters of continuous laser welding of cast iron

Dmitry Ilyushkin [a, *], ***Valery Soldatov*** [b], ***Oleg Petrakov*** [c], ***Irina Kotlyarova*** [d]

Bryansk State Technical University, 7, 50 Let Oktyabrya Boulevard, Bryansk, 241035, Russian Federation

[a] https://orcid.org/0000-0002-4265-9570, shirke@mail.ru, [b] https://orcid.org/0000-0001-6318-5522, soldat-tu@bk.ru,
[c] https://orcid.org/0000-0003-4937-1411, typeofpeople@mail.ru, [d] https://orcid.org/0000-0001-6162-0199, ikotlyarova@list.ru

ARTICLE INFO

Article history:
Received: 19 January 2021
Revised: 26 January 2021
Accepted: 05 August 2021
Available online: 15 September 2021

Keywords:
Laser welding
Cast iron
Regression analysis
Grey Relational Analysis
Optimization

Acknowledgements
Research were conducted at core facility "Structure, mechanical and physical properties of materials".

ABSTRACT

Introduction. Cast iron extremely poorly tolerate thermal welding cycles, and therefore it is necessary to choose carefully the technological parameters. The main parameters of continuous laser welding are: the power of laser radiation, the welding speed, the parameters of the focusing system. **The aim of the work** is to determine the optimal power and speed of continuous laser welding of cast iron, depending on the geometry of the weld. **In this paper,** the welding seams obtained on samples of gray alloyed cast iron with a pearlitic metal base, using an LS-1 ytterbium fiber laser, are studied. **Research methods.** The geometric parameters of the joints were quantified in the program for quantitative analysis and image processing ImageJ. The obtained data were processed by regression analysis. To optimize the process parameters, an orthogonal plan of the passive experiment was developed, including nine experiments in which the factors varied at three equally spaced levels. The quality parameters in the passive experiment were the geometric dimensions of the weld pool and the size of the quenched zone. To solve the optimization problem, we used the methods of gray relational analysis and linear programming. **Results and Discussions.** The obtained regression models explain a significant proportion of the variance of the dependent variables, the regression coefficients, as well as the models themselves, are statistically significant, which indicates a close linear relationship between the seam geometry and the process parameters. The calculated shape of the weld pool depending on the radiation power and welding speed shows that the required welding seam of the required dimensions can be obtained at various process parameters which allow solving a multi-criteria optimization problem. The gray relational evaluation of the geometric parameters of the seam shows that the most correct parameters in terms of obtaining the seam of the maximum depth with the minimum width, convexity (concavity) and the quenched zone are the minimum power and maximum welding speed. The calculation of the optimal radiation power and welding speed depending on the seam depth showed that welding of small thicknesses is optimally carried out with minimal power, and the seam depth is adjusted by changing the beam speed. Welding of large thicknesses is optimal at high speed, and to increase the depth of the seam, the power must increase.

For citation: Ilyushkin D.A., Soldatov V.G., Petrakov O.V., Kotlyarova I.A. On the issue of selecting and optimizing parameters of continuous laser welding of cast iron. *Obrabotka metallov (tekhnologiya, oborudovanie, instrumenty) = Metal Working and Material Science*, 2021, vol. 23, no. 3, pp. 20–30. DOI: 10.17212/1994-6309-2021-23.3-20-30. (In Russian).

Introduction

Laser technology is a relatively new technological method that finds application in welding, cutting, surface treatment and hardening. Due to its versatility, laser can become a promising instrument in single and small-scale production.

Compared to electric arc welding, which is the most widespread, laser welding has a number of advantages: the seam is not contaminated by the electrode material, a number of harmful impurities (sulfur, oxygen, nitrogen, etc.) evaporate from the melt, the tendency to form hot and cold cracks is reduced,

*** Corresponding author**
Ilyushkin Dmitry A., Ph.D. (Engineering), Associate Professor
Bryansk State Technical University,
7, 50 Let Oktyabrya Boulevard,
241035, Bryansk, Russian Federation
Tel.: 8 (4832) 58-82-61, **e-mail:** shirke@mail.ru

and crystallization conditions improve, which increases the weld properties. In addition, productivity significantly rises [1].

Laser technologies for processing cast iron can be used for producing welded cast products, repair, fix defects, surface microalloying and improving its performance [2].

Cast irons have a porous structure. Graphite inclusions that violate its metal base continuity complicate the welding process, lead to porosity and defects in the weld [3, 4]. While melting and subsequent crystallization in the melt-pool, the white cast iron structure is formed [5–7]. In this regard, cast irons endure thermal welding cycles extremely poorly: structure heterogeneity and local stresses lead to brittleness [8].

Depending on the laser operating parameters, it is customary to distinguish between two characteristic modes of laser welding: welding of small thicknesses (up to 1 mm) and welding with a deep penetration (more than 1 mm). The principal difference of the first group is the modes that provide only melting the material without its intense evaporation. The processes in the melt-pool are unsteady and unstable. Deep penetration welding is accompanied by forming the melt turbulent flows and the steam-gas channel [9].

The geometric parameters of the melt-pool (depth, width and its ratio) are some of the weld quality indicators and differ for the two described welding modes. The main technological parameters that ensure the melt-pool geometry are radiation power, welding speed and focusing system parameters [1].

At low speeds the steam-gas channel has a cylindrical shape, the aspect ratio of the melt-pool can be quite large, while at high speeds the aspect ratio is low [10].

To select the optimal parameters of the welding process, optimize the cast iron structure, and increase energy efficiency, mathematical models of the process are needed.

The models based on the energy equations and momentum balance make it possible to quantitatively estimate the dependence of the melting zone penetration and other geometric characteristics of the weld seams on the main technological parameters of welding [11–13]. However, the optimal welding speed doesn't only depend on the radiation parameters, but also on the structure of the materials to be welded, for example, on the graphite phase behaviour when welding cast iron. At extremely low or too high speeds, the process becomes unstable. Thus, in [14] it is shown that at a high radiation power and a relatively short time of laser action, a significant part of graphite in the melting zone structure is retained. The time increase in a high-power laser exposure leads to explosive evaporation and graphite sublimation, which is accompanied by the crater formation on the weld surface. These phenomena significantly complicate the mathematical description of the process.

In work [15] it is shown that to build an effective model for forecasting the welded seam quality, it is necessary to consider many parameters. As an example, a simplified predictive model based on an artificial neural network is presented, which demonstrates possible and promising indicators for forecasting the welding quality of a low-carbon galvanized steel sheet.

The work [16] provides qualitative data on influencing two process parameters on the geometric parameters of the bath (Table 1). In addition, there are recommendations for choosing the optimal parameters for some types of steel and non-ferrous metal alloys.

Table 1

Influence of two laser welding parameters on various weld pool geometry parameters

Geometry parameter	Process parameter	
	Laser power	Welding speed
Weld pool depth	+	−
Weld pool width	+	−
Weld pool depth/width ratio	it is not stated in the work	+
Weld pool length	+	−
Keyhole radius	+	−
Cooling rate	−	+
Weld pool surface area	+	−
Vaporization rate	+	it is not stated in the work

In [17], it is shown that the melting zone cross-sectional area (the weld pool geometry) while welding Ni-resist cast iron is proportional to the laser exposure time: as the beam speed decreases, the melt mass loss as a result of its evaporation increases.

In work [18], by the method of planning a factorial experiment, mathematical models are constructed that relate the weld pool depth with the laser power, welding speed and a focal length. A significant difference in the coefficient estimations for welding steels of two different grades is shown. This indicates the absence of any universal statistical models for evaluating the weld pool geometry; these models are applicable only to the dataset on which it is built.

The cast iron structure with the same chemical composition can have an unpredictable and chaotic distribution of graphite inclusions of various shapes and sizes. The behaviour of the graphite phase while melting, as it is noted above, depends on the welding mode, which ultimately determines the weld seam main characteristics and quality.

Thus, to increase the process energy efficiency and provide the weld pool required geometry for each variant of the technical process, it is necessary to select the optimal welding modes. This problem is effectively solved using mathematical models. In this regard, it becomes necessary to study and quantify the weld pool geometry while welding cast iron with different structure, depending on the technological parameters of the process.

The aim of the work is to build a mathematical model of welding cast iron with lamellar graphite and determine the optimal power and welding speed depending on the weld pool geometry.

Work tasks:

1. Carrying out an experiment and regression analysis of the weld pool geometry dependence on welding modes.
2. Studying the cast iron structure in the melting zone.
3. Gray relational estimation of the weld pool geometric parameters.
4. Calculating the optimal radiation power and welding speed depending on the weld pool geometry.

Research methodology

For the experiment, cylindrical specimens with a 30-mm diameter and a 10-mm height were made from grey unalloyed cast iron with a pearlite metal base. Cast irons with such a structure have a good hardenability, which simplifies assessing the effect of welding parameters on the heat affected zone extent. Laser treatment to simulate the welding process was carried out on an LS-1 ytterbium fibre laser in accordance with the plan (Table 2). The focal length in the experiment did not vary and was 120 mm.

At a distance excluding thermal influence, 4 tracks were melted on each specimen. The samples were studied by traditional metallographic methods. The study was carried out on a computerized complex created on the basis of a Leica DM IRM metallographic microscope. The quantitative assessment of the geometric parameters of the weld seams was carried out in the programme ImageJ used for a quantitative analysis and image processing.

Table 2

Design of experiment

Sample	Laser power, kW	Welding speed, mm/s
1	0,7	50
2	1,3	20
3	0,575	35
4	1,0	56
5	1,0	14

Results and discussion

The laser action zone consists of 2 layers: a melting zone and a zone quenched from a solid phase (Fig. 1). The tempering zone on the obtained samples was not identified.

Graphite inclusions partially or completely (depending on the processing mode) dissolved in the liquid phase, crystallization proceeded according to the iron-carbon metastable diagram without releasing free graphite. Due to the high crystallization rate, releasing excess phases was suppressed; as a result, the entire melt passed into a finely dispersed mixture of austenite and cementite (quasi-eutectic ledeburite).

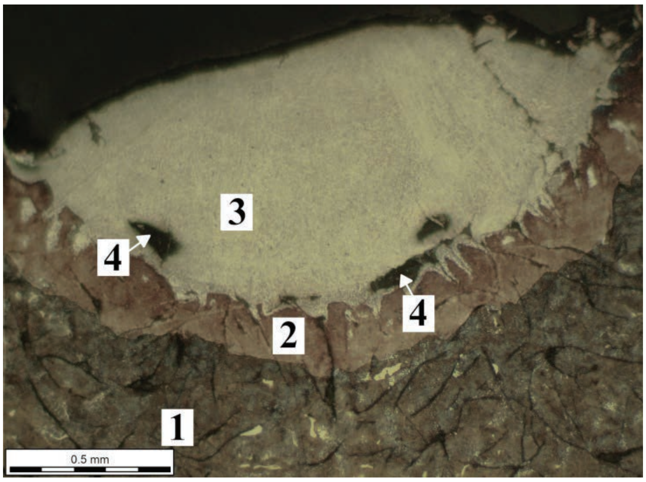

Fig. 1. Microstructure of sample No. 5:
1 – source material; *2* – hardening area; *3* – penetration area; *4* – welding defect

An accurate analytical description of the hydrodynamics processes, heat and mass transfer in the weld pool, affecting the weld geometry is not an easy task in view of its complexity. Therefore, to optimize the welding parameters, it is convenient to make simplified mathematical models. For this aim, a regression analysis of the obtained data was carried out, the results of which are presented in table. 3

Regression models explain a significant proportion of the dependent variable dispersion. Regression coefficients, like the model itself, are statistically significant. Regression prerequisites for each model are met. All this testifies to the close linear relationship between the weld geometry and process parameters.

High laser power and at the same time high welding speed provide the melt-pool smallest width and obtain "a knife fusion" penetration (Fig. 2). In this way, narrow, deep weld seams can be obtained. Due to the low heat capacity, graphite inclusions are heated to a significantly higher temperature than the base metal. The metal vaporisation and the graphite sublimation cause excessive pressure in the weld channel, which leads to the melt displacement from the melt-pool, as a result of which discontinuities of significant size are formed in this area, mainly in the weld root part. In this case, the bead convexity considerably increases.

Reducing the laser speed at a high laser power increases the weld pool width and decreases the penetration. As a result, a wide bead with a small convexity is formed. The volumes of discontinuities in the melting zone are significantly reduced (Fig. 1). However, decreasing the penetration ratio to the weld width increases the level of tensile stresses arising from the cast iron shrinkage in the weld pool. Reducing the

Table 3

Regression analysis results

Statistics	Dependent variables			
	Width, mm	Penetration, mm	Convexity, mm	Hardening area, mm
Laser power, kW	1.127*** (Std. Error 0.112)	2.889*** (Std. Error 0.141)	0.798** (Std. Error 0.188)	0.083*** (Std. Error 0.017)
Welding speed, mm/s	–0.023*** (Std. Error 0.002)	0.021*** (Std. Error 0.002)	0.015*** (Std. Error 0.003)	–0.001** (Std. Error 0.001)
Intercept	1.170*** (Std. Error 0.142)	–1.979*** (Std. Error 0.180)	–1.034** (Std. Error 0.278)	0.079** (Std. Error 0.022)
Observations	20	20	10	20
R^2	0.966	0.961	0.794	0.765
Adjusted R^2	0.962	0.956	0.735	0.737
Residual Std. Error	0.115 (df = 17)	0.145 (df = 17)	0.127 (df = 7)	0.018 (df = 17)
F-statistic	240.182*** (df = 2; 17)	209.358*** (df = 2; 17)	13.484*** (df = 2; 7)	27.64*** (df = 2; 17)

Note: * $p < 0.1$; ** $p < 0.05$; *** $p < 0.01$.

Fig. 2. Microstructure of sample No. 4

heating and cooling rates increases a hardening zone from the solid phase, which has a brittle martensitic base. Together, these factors add to the risk of transverse cracking in long weld seams.

Reducing the laser power and welding speed allows providing cast iron melting without its intense boiling and vaporisation. In this case, complete dissolution of graphite inclusions is possible.

The weld bead of the required dimensions can be obtained at various powers and welding speeds (Fig. 3). The choice of the optimal technological parameters that ensure a high-quality seam is a multi-criteria optimization problem. On the other hand, it would be desirable to carry out a welding process at a minimum power and at a maximum speed.

In the optimization problems for several dependent variables (penetration, width, weld convexity, hardening zone thickness), assessing a certain complex quality indicator is required. To resolve the issue of power and welding speed optimal levels, the method of grey relational analysis was chosen [19, 20]. An orthogonal matrix (9×2) was constructed, which was a passive experiment, consisting of 9 experiments, in which the factors varied at 3 equidistant levels. The experimental design and the geometric parameters of the weld seams calculated using regression models (Table 2) are presented in Table 4.

The initial data for the analysis should be normalized. The melting zone penetration was normalized in accordance with the “bigger is better” principle according to the formula:

$$x_{ij} = \frac{\max_j y_{ij} - y_{ij}}{\max_j y_{ij} - \min_j y_{ij}}$$

where y_{ij} – is the value of the *i-th* parameter (penetration of the melting zone) in the *j-th* experiment.

Other geometrical parameters of the weld seam are suitable for the “less is better” characteristic:

$$x_{ij} = \frac{y_{ij} - \min_j y_{ij}}{\max_j y_{ij} - \min_j y_{ij}}$$

The degree of discrepancy between the ideal (best) and experimental settings is expressed by the value of gray relational coefficients, which are calculated by the formula:

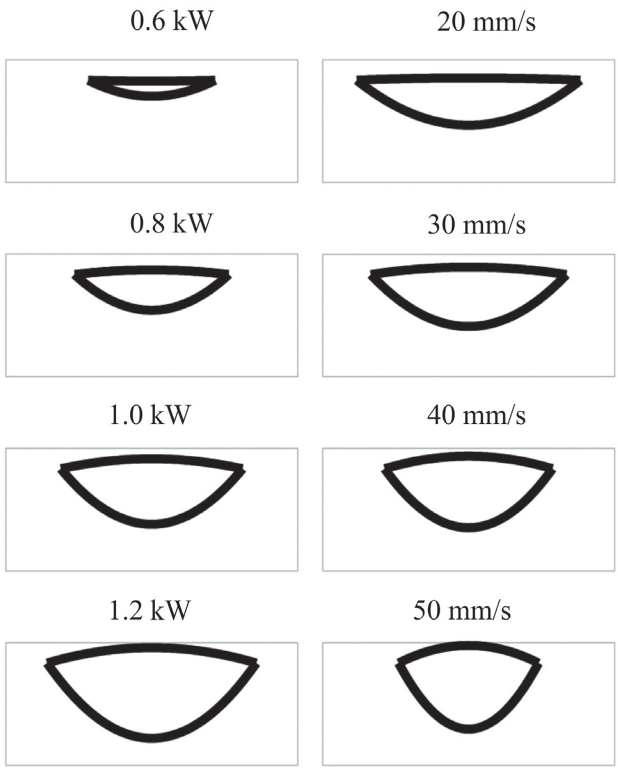

Fig. 3. Calculated shape of the weld seam depending on laser power and welding speed:
a – welding speed 35 mm/s; *b* – laser power 1 kW

Table 4

Orthogonal array, natural values and corresponding response values

№	x_1*	x_2*	Laser Power, kW	Welding speed, mm/s	Penetration (y_1), mm	Width (y_2), mm	Convexity (y_3)**, mm	Hardening area (y_4), mm
1	1	1	0.6	14	0.04	1.53	–0.34	0.12
2	1	2	0.6	35	0.48	1.04	–0.03	0.10
3	1	3	0.6	56	0.91	0.56	0.29	0.08
4	2	1	0.95	14	1.05	1.92	–0.06	0.15
5	2	2	0.95	35	1.49	1.44	0.25	0.13
6	2	3	0.95	56	1.92	0.96	0.57	0.11
7	3	1	1.3	14	2.07	2.31	0.22	0.18
8	3	2	1.3	35	2.5	1.83	0.53	0.16
9	3	3	1.3	56	2.93	1.35	0.85	0.14

Note: * coded values of laser power and welding speed; ** a minus means concavity of the weld seam

$$\xi_{ij} = \frac{\min_i \min_j \left|x_i^0 - x_{ij}\right| + \zeta \max_i \max_j \left|x_i^0 - x_{ij}\right|}{\left|x_i^0 - x_{ij}\right| + \zeta \max_i \max_j \left|x_i^0 - x_{ij}\right|}$$

where x_i^0 – is an ideal normalized result of the *i-th* parameter, $x_i^0 = 1$; ζ – is the coefficient of difference, in this study it is taken $\zeta = 0,5$.

The grey relational grade is determined by averaging the grey relational coefficients:

$$\gamma_j = \frac{1}{m}\sum_{i=1}^{m}\xi_{ij}$$

Grey relational grades averaged over the factor variation levels are shown in Fig. 4. The horizontal line on the graph corresponds to the average relational grade in the experiment.

The graph in Fig. 4 and the data in table 5 show that the most attractive parameters from the viewpoint of obtaining a maximum penetration weld seam with a minimum width, convexity (concavity) and hardening zone are the minimum power and maximum welding speed, which corresponds to mode No. 3. In addition, at the given parameters, the process maximum productivity and economy are achieved.

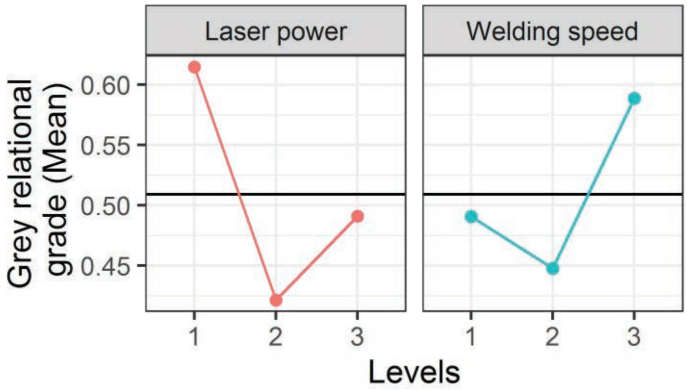

Fig. 4. Main effects plot for Grey relational grade

Table 5

Grey relational grade results

№	ξ_1	ξ_2	ξ_3	ξ_4	γ	Rank
1	0.48	1	0.58	0.33	0.6	2
2	0.61	0.62	0.7	0.33	0.56	4
3	1	0.4	1	0.33	0.68	1
4	0.33	0.62	0.36	0.37	0.42	8
5	0.33	0.33	0.33	0.33	0.33	9
6	0.63	0.33	0.55	0.52	0.51	5
7	0.33	0.52	0.33	0.63	0.45	6
8	0.36	0.36	0.33	0.73	0.45	7
9	0.53	0.33	0.44	1	0.57	3

Let us require fulfilling these conditions in the optimization problem:

$$\begin{cases} p \rightarrow \min \\ v \rightarrow \max \\ d - 1.979 = 2.889p + 0.021v \\ m + 0.079 = 0.083p - 0.00v \\ d + m = t \\ 0.6 \le p \le 1.3 \\ 14 \le v \le 56 \end{cases}$$

where p – is laser power , kW; v – is welding speed, mm/s; d – is melting zone penetration, mm; m – is hardening zone size from the solid phase, mm; t – is weld seam penetration, mm. Restrictions on the penetration of the melting and hardening zones were taken in accordance with the obtained regression models (Table 2), the intervals for varying the power and speed were taken in accordance with the levels of factors adopted during the experiment (Table 1).

The problem was solved by the linear programming method. The solution is presented in the form of a graph in Fig. 5.

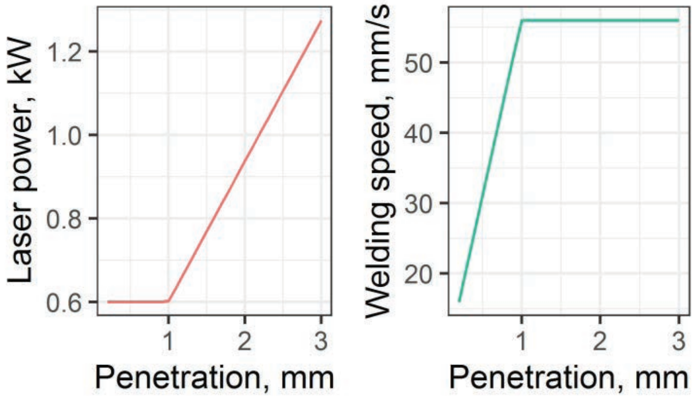

Fig. 5. Optimal laser power and welding speed depending on the weld penetration

The dependence in Fig. 5 shows that welding of small thicknesses (up to 1 mm) is optimally carried out with a minimum power, and the weld seam penetration is regulated by changing the laser speed. A high speed is optimal when welding large thicknesses (over 1 mm), while the optimum power increases linearly with raising the seam penetration. At a depth of more than 3 mm, the problem has no solution; it is impossible to obtain such a weld seam with the accepted intervals of varying technological parameters.

Conclusion

There are optimum laser welding parameters for each material. In this work the authors use the methods of regression analysis, gray relational analysis, linear programming to identify the dependence, which makes it possible to have a reasonable choice of technological parameters of continuous laser welding (laser power, welding speed) of cast iron to a 3-mm depth. It is found that welding of small thicknesses is optimal at a minimum power, welding of large thicknesses is optimal at a maximum speed. The findings in their pure form are valid for lamellar graphite cast irons having a pearlitic metal base when welding with an ytterbium fibre laser with a power of 0.6 to 1.3 kW at a speed of 14 to 56 mm/s with a 120-mm focal length.

References

1. Olson D.L., Siewart T.A., Liu S., Edwards G.R. *ASM Handbook*. Vol. 6. *Welding, brazing, and soldering*. ASM International, 1993. 2873 p.

2. Gusev A.A. Perspektivy impul'snogo lazernogo legirovaniya i naplavki [Outlooks for pulse-laser alloying and pad welding]. *Izvestiya Samarskogo nauchnogo tsentra Rossiiskoi akademii nauk = Proceedings of the Samara Scientific Center of the Russian Academy of Sciences*, 2012, vol. 14, no. 6, pp. 247–253.

3. Lin C.-M., Chandra A.S., Morales-Rivas L., Huang S.-Y., Wu H.-C., Wu Y.-E., Tsai H.-L. Repair welding of ductile cast iron by laser cladding process: microstructure and mechanical properties. *International Journal of Cast Metals Research*, 2014, vol. 27, iss. 6, pp. 378–383. DOI: 10.1179/1743133614Y.0000000126.

4. Fu Q., Yi P., Xu P., Fan C., Yang G., Liu D., Shi Y. Microstructure formation and fracturing characteristics of grey cast iron repaired using laser. *The Scientific World Journal*, 2014, vol. 2014, p. 541569. DOI: 10.1155/2014/541569.

5. Piątkowski J., Grabowski A., Czerepak M. The influence of laser surface remelting on the microstructure of EN AC-48000 cast alloy. *Archives of Foundry Engineering*, 2016, vol. 16, iss. 4, pp. 217–221. DOI: 10.1515/afe-2016-0112.

6. Matveev Yu.I., Kazakov S.S. Formirovanie struktur serogo chuguna v zone lazernogo vozdeistviya [Formation of structures of grey pig-iron in the zone of laser influence]. *Vestnik NGIEI = Bulletin NGIEI*, 2011, vol. 2, no. 1 (2), pp. 41–53.

7. Benyounis K.Y., Fakron O.M.A., Abboud J.H., Olabi A.G., Hashmi M.J.S. Surface melting of nodular cast iron by Nd-YAG laser and TIG. *Journal of Materials Processing Technology*, 2005, vol. 170, iss. 1, pp. 127–132. DOI: 10.1016/j.jmatprotec.2005.04.108.

8. Bhatnagar R.K., Gupta G. A review on weldability of cast iron. *International Journal of Scientific and Engineering Research*, 2016, vol. 7, iss. 5, pp. 126–130. Available at: https://www.ijser.org/researchpaper/A-REVIEW-ON-WELDABILITY-OF-CAST-IRON.pdf (accessed 13.08.2021).

9. Kou S. *Welding metallurgy*. John Wiley & Sons, 2003. 468 p.

10. Fabbro R. Depth dependence and keyhole stability at threshold, for different laser welding regimes. *Applied Sciences*, 2020, vol. 10, iss. 4, p. 1487. DOI: 10.3390/app10041487.

11. Panchenko V.Ya., ed. *Lazernye tekhnologii obrabotki metallov: sovremennye problemy fundamental'nykh issledovanii i prikladnykh razrabotok* [Laser technologies of metal processing: modern problems of fundamental research and applied developments]. Moscow, Fizmatlit Publ., 2009. 664 p. ISBN 978-5-9221-1023-5.

12. Lankalapalli K.N., Tu J.F., Gartner M. A model for estimating penetration depth of laser welding processes. *Journal of Physics D: Applied Physics*, 1996, vol. 29, iss. 7, pp. 1831–1841. DOI: 10.1088/0022-3727/29/7/018.

13. Tan W., Bailey N.S., Shin Y.C. Investigation of keyhole plume and molten pool based on a three-dimensional dynamic model with sharp interface formulation. *Journal of Physics D: Applied Physics*, 2013, vol. 46, iss. 5, p. 055501. DOI: 10.1088/0022-3727/46/5/055501.

14. Dikova T., Stavrev D. Behaviour of graphite in laser surface hardening of irons. *Machines, Technologies, Materials*, 2007, vol. 4–5, iss. 9, pp. 98–101.

15. Oussaid K., El Ouafi A., Chebak A. Experimental investigation of laser welding process in overlap joint configuration. *Journal of Materials Science and Chemical Engineering*, 2019, vol. 7, pp. 16–31. DOI: 10.4236/msce.2019.73002.

16. Fotovvati B. Wayne S.F., Lewis G. Asadi E., Ferro P. A review on melt-pool characteristics in laser welding of metals. *Advances in Materials Science and Engineering*, 2018, vol. 2018, p. 4920718. DOI: 10.1155/2018/4920718.

17. Gilev V.G., Morozov E.A., Purtov I.B., Rusin E.S. Issledovanie mikrostruktury i mikrotverdosti zon lazernogo oplavleniya chuguna nirezist ChN16D7GKh [Microstructure and microhardness research of Ni-rezist cast iron after laser surface melting]. *Izvestiya Samarskogo nauchnogo tsentra Rossiiskoi akademii nauk = Proceedings of the Samara Scientific Center of the Russian Academy of Sciences*, 2014, vol. 16, no. 6, pp. 227–233.

18. Metzbower E.A. Penetration depth in laser beam welding. *Welding Research Supplement*, 1993, vol. 407, pp. 403–407.

19. Ravikumar S.M., Vijian Dr.P. Optimization of weld bead geometry in Shielded Metal Arc Welding using Taguchi Based Grey Relational Analysis. *International Journal of Mechanical and Mechatronics Engineering*, 2014, vol. 14, iss. 4, pp. 86–91.

20. Khaimovich A.I., Sanchugov V.I., Stepanenko I.S., Smelov V.G. Optimizatsiya selektivnogo lazernogo splavleniya metodom otsenki mnozhestvennykh parametrov kachestva v dvigatelestroenii [Optimization of selective laser melting by evaluation method of multiple quality characteristics]. *Izvestiya Samarskogo nauchnogo tsentra Rossiiskoi akademii nauk = Proceedings of the Samara Scientific Center of the Russian Academy of Sciences*, 2018, vol. 20, no. 6, pp. 41–46.

Conflicts of Interest

The authors declare no conflict of interest.